ELSEVIER

Journal of Hazardous Materials 55 (1997) 39–60

JOURNAL OF HAZARDOUS MATERIALS

Scale-up aspects of the Lasagna™ process for in situ soil decontamination

Sa.V. Ho [a,*], Christopher J. Athmer [a], P. Wayne Sheridan [a], Andrew P. Shapiro [b]

[a] *Monsanto Company, 800 N. Lindbergh Blvd., St. Louis, MO 63167, USA*
[b] *GE Corporate R&D, P.O. Box 8, Schenectady, NY 12301, USA*

Abstract

A novel integrated in situ remediation technology called Lasagna™ is being developed coupling electrokinetics with in situ treatment zones. The first field test of the process was successfully completed in May of 1995 at a DOE site in Paducah, KY, which has clayey soil contaminated with trichloroethylene. This paper focuses on the scale-up characteristics of the Lasagna process from bench to pilot scale. The study was critical for developing predictive models that aided in the design of the field test. Key parameters such as electrokinetic characteristics, soil temperature, cathode effluent pH and conductivity, and treatment zone spacing were evaluated under controlled conditions. Experiments were conducted with both kaolin clay and the actual Paducah soil using various treatment zone configurations. The obtained data support the feasibility of scaling up this technology with respect to electrokinetic parameters such as electro-osmotic permeability and energy consumption. The removal of the model organic compound p-nitrophenol from the soil was also very efficient (98% in one pass) in the pilot unit. A mathematical model was developed that successfully predicted the temperature rises observed in the soil as a function of the applied voltage gradients. © 1997 Elsevier Science B.V.

Keywords: Lasagna™ process; Soil decontamination; Electrokinetics

1. Introduction

A novel in situ technology is being developed for cleanup of contamination in low-permeability soils or heterogeneous soils containing low-permeability zones. The approach involves the synergistic coupling of electrokinetics [1–9] with in situ treatment processes. The general concept is to use electrokinetics to transport contaminants from

* Corresponding author.

PII S0304-3894(97)00016-2

the soil into "treatment zones" where the contaminants are removed from the pore water by sorption, immobilization or degradation. This integrated technology has been described elsewhere [10]. Briefly, it consists of the following components.

(a) Create permeable zones in close proximity sectioned through the contaminated soil region, and turn them into "treatment zones" (e.g. sorption, immobilization, degradation) by introducing appropriate materials (sorbents, catalytic agents, microbes, oxidants, buffers, etc.).

(b) Utilize electrokinetics to transport contaminants from the soil into the treatment zones.

With the in situ treatment approach, the cathode effluent (at alkaline pH) can be directly recycled back to the anode side (at acidic low pH), thus providing a convenient means for pH neutralization as well as simplifying water management. Additionally, liquid flow can be periodically reversed, if needed, simply by switching the electrical polarity. This mode would enable multiple passes of the contaminants through the treatment zones for complete sorption/destruction. The periodic polarity reversal could also help minimize complications associated with long-term operation of uni-directional electrokinetic processes, such as highly non-uniform potential and pH distribution in the soil matrix [4,7,9,10].

Electrodes and treatment zones can be of any orientation depending upon the emplacement technology used and the site/contaminant characteristics. Schematic diagrams of two typical configurations, horizontal and vertical, are shown in Fig. 1. The process has been called "Lasagna™" [10,11] due to the layered configuration of electrodes and treatment zones. Generally, horizontal fractures could be formed in overconsolidated clays employing vertical pressuring scheme for installation of horizontal electrodes and treatment zones. Hydrofracturing [12] is such a method and is effective for dealing with deep contamination. For shallow contamination (< 50 feet) and especially if the soil is not overconsolidated, vertical treatment approach using sheet piling or trenching may be more appropriate.

Conceptually, the Lasagna technology exhibits a high degree of flexibility in the treatment process used, which can incorporate mixtures of different treatment materials in the same treatment zone or utilizes functionally distinct treatment zones. The technology can thus be potentially effective for treating organic (e.g., chlorinated solvents) or inorganic (e.g., heavy metals) contamination as well as mixed wastes. With electrokinetics as the mechanism for contaminant transport, the technology is well suited for treating contaminated low permeability soils (clayey, silty soils) or heterogeneous soils (clay lens in permeable soils).

A consortium of industry (DuPont, GE and Monsanto) has been formed and is collaborating with two federal agencies (EPA and DOE) to combine expertise and resources for accelerating the development of this technology. A field test of the process was successfully completed at a DOE site in Paducah, KY, which has clayey soil contaminated with trichloroethylene (TCE). In support of this program, we studied the movement of water and contaminants through kaolin clay and Paducah soil using the Lasagna™ process. The process was extensively studied at the bench level, then scaled up in a laboratory pilot unit. The pilot-scale experiments played an important role in the development of models and designs for the field tests. Electrokinetic characteristics, soil

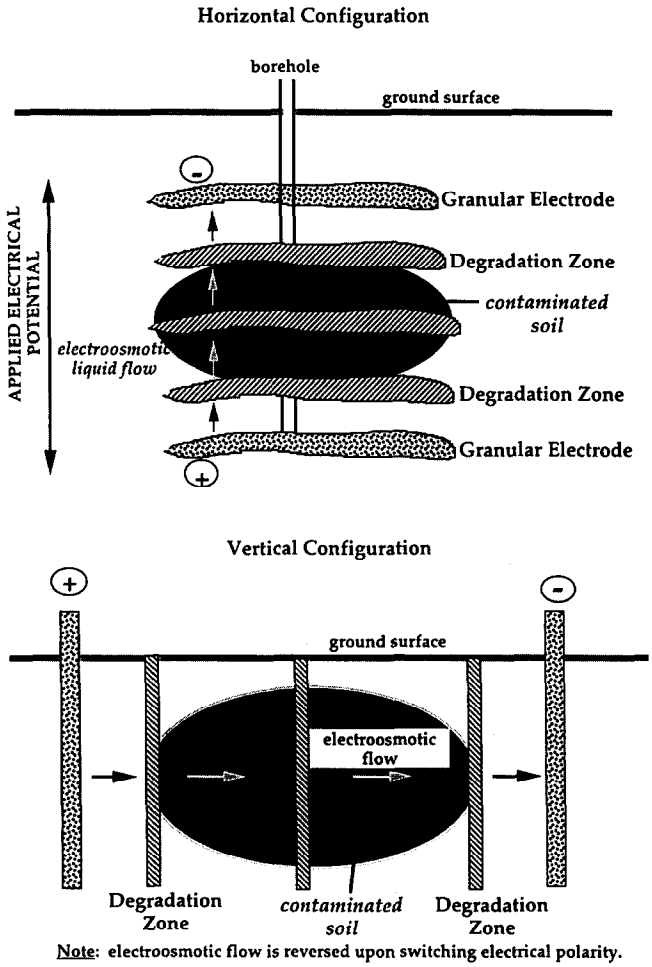

Fig. 1. Diagram showing two typical configurations of the Lasagna process.

temperature, cathode effluent pH and conductivity, and ion electromigration were evaluated under controlled conditions. This paper focuses on the scale-up aspects of the Lasagna process from bench to pilot scale. Bench-scale study of various Lasagna configurations including heterogeneous soil matrices and coupling electrokinetics with in situ biotreatment has been reported elsewhere [10].

2. Materials and methods

2.1. Bench-scale

The bench-scale unit has been described in detail elsewhere [10]. Briefly, the electrokinetic cell was made from clear plastic tube, 10 cm ID (81 cm^2 cross-sectional area). Kaolinite or Paducah soil was sandwiched between sand and/or granular acti-

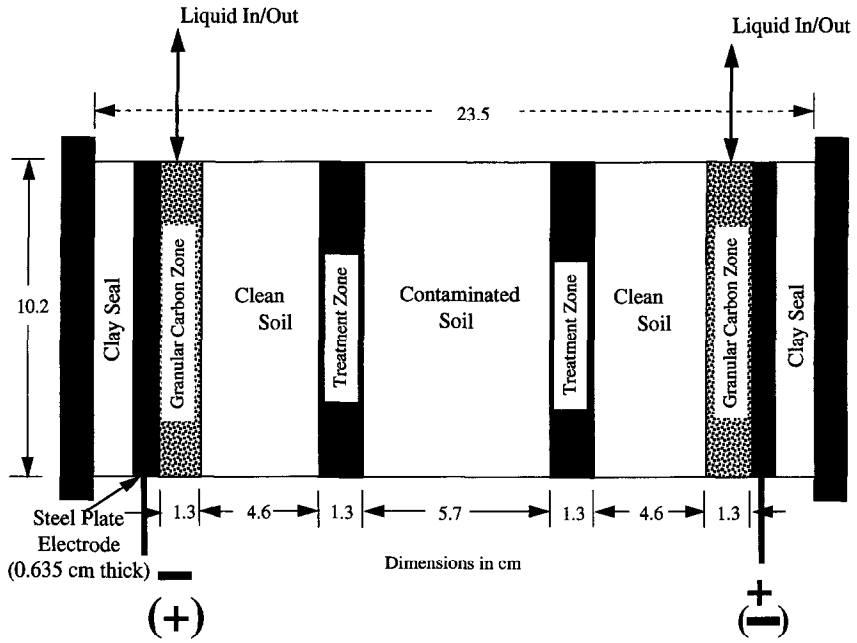

Fig. 2. Schematic diagram of the bench-scale unit.

vated carbon "treatment zones". The outermost treatment zones functioned primarily as the hydraulic input and output zones. Well water or recycled cathode fluid was introduced at the anode treatment zone under constant head using a Marriotte bottle. The cathode fluid was expelled at the top of the cathode treatment zone and put into the Marriotte bottle. A plug of glass wool in the inlet/outlet fittings prevented solid material from leaving the unit. The center treatment zones contained some mixture of sand and GAC. The center "contaminated soil" section was approximately 6.5 cm long and outer soil zones were approximately 4.6 cm long. The electrodes were made of 0.635 cm thick steel plates with stainless steel rods screwed into the edge of the steel plates for connections to the power supply. The distance between the plate electrodes was 18 cm. Fig. 2 shows a diagram of the bench-scale electrokinetic cell.

2.2. *Pilot-scale*

A pilot-scale Lasagna unit (Fig. 3) was constructed from a Nalgene® polyethylene tub (122 cm long by 61 cm wide by 61 cm deep) to simulate the vertical Lasagna configuration to be used at the DOE Paducah site. Electrodes were made of steel plates 0.635 cm thick, 60 cm wide and 51 cm tall. These electrodes were placed at each end of the polyethylene tub and were connected to the power leads by 12 gauge wire. Immediately in front of each electrode was a permeable zone to allow inflow and outflow of liquid to the electrode region. The permeable zones were constructed the same way as the treatment zones described below.

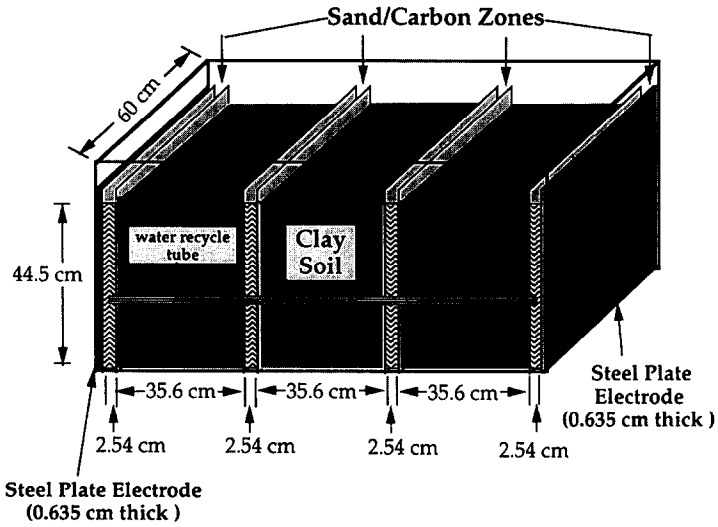

Fig. 3. Schematic diagram of the pilot unit.

Treatment zones were constructed in three configurations. In the kaolinite experiments, each treatment zone consisted of 13.6 kg of medium sand and 100 g of granular activated carbon (GAC). Sand and carbon in each zone were contained between two porous polypropylene sheets measuring 0.32 cm thick, 60 cm wide, 51 cm tall and approximately 2.54 cm apart. There were a total of four treatment zones, two in the center of the bed and two in front of the electrodes. The distance between the two adjacent treatment zones was about 36 cm.

Subsequent runs used treatment zones constructed by Wickdrain Inc. These treatment zones were made by gluing egg-crate polyethylene sheets to steel frames which had holes drilled to allow water passage. The wickdrain was then wrapped with a geotextile and filled with 100% GAC. These zones were placed 36 cm apart and were 60 cm wide by 61 cm tall. The last Paducah soil pilot experiment used Monsanto Hydroway® construction wicking material filled with GAC and had a single treatment zone in the center in order to increase the treatment zone spacing to 53.3 cm.

Once the treatment zones were installed in the unit, Georgia kaolinite clay (air-dried, air-floated kaolinite obtained from Thiele Kaolinite Co., Wrens, GA) or Paducah soil was placed in the unit between the treatment zones. The first 2 pilot runs were prepared with kaolin clay packed to a depth of 43.2 cm. Kaolin powder was hydrated with tap water in a wheelbarrow to a water content of 37.5 wt%. All other pilot runs used Paducah soil obtained from the Western Kentucky Wildlife Management Area (WKWMA), adjacent to the DOE Paducah Plant site where the field trial was conducted. Some characteristics of kaolinite and the Paducah soil are listed in Table 1. The Paducah soil is classified as clay loam, with fairly low organic content (0.2%) and much higher cation exchange capacity (13.4 meq per 100 g) than kaolinite (1.1 meq per 100 g).

Table 1
Characteristics of kaolin clay and Paducah soil

Parameter	Unit	Kaolinite	Paducah
Soil type		clay	clay loam
Sand	%	0	22
Silt	%	0	46
Clay	%	100	32
Bulk density	g cm^{-3}	1.65	2.0
Porosity	cm^3 cm^{-3}	0.62	0.4
Moisture	%	37.5	20
Cation exchange capacity	meq per 100 g	1.1	13.4
Organic carbon content	%	0	0.2
Estimated hydraulic conductivity	cm s^{-1}	10^{-8}	10^{-7}–10^{-8}

After the soil was packed in the unit for the first pilot run, holes were drilled into the side of the tub to allow access to the treatment zones for sampling. Water recycling from the cathode zone back to the anode zone occurred by gravity through 0.635 cm OD polyethylene tubing on the outside of the tub that connected the two zones (Fig. 3). No pump was used.

For studying contaminant transport, five sausage-like units of paranitrophenol (PNP) contaminated clay were placed in the center section of the pilot unit. The sausages, approximately 25 cm long and 3.8 cm in diameter, were uniformly contaminated to 370 μg PNP per g wet soil for a total of 0.94 g PNP. Dialysis membrane was used to encase the PNP contaminated clay for convenient retrieval and analysis during and after the test. Four of the five sausages were placed horizontally in the center clay zone reaching nearly from treatment zone to treatment zone and centered in the four quadrants. The fifth sausage was placed vertically in the unit, in the center of the middle clay zone (Fig. 4).

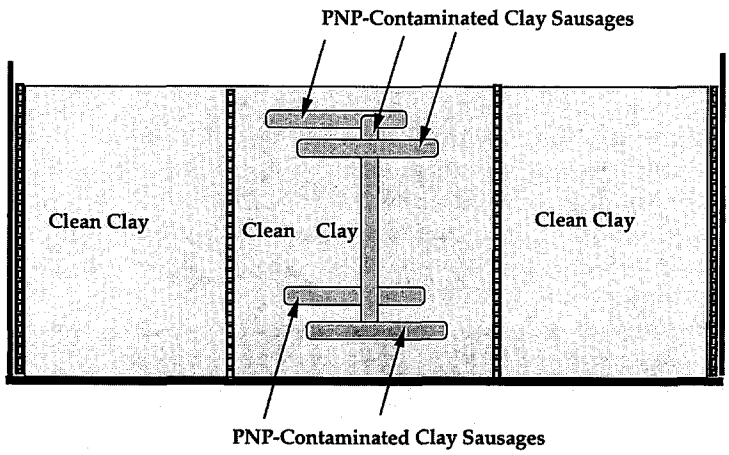

Fig. 4. Orientation of the five PNP-contaminated clay sausages.

A type "J" thermocouple was installed near the center of the unit to monitor temperature effects on the last paducah soil test. The temperature was read using a hand held digital thermometer (Fluke Model 51) calibrated at the ice point (0°C).

2.3. Analytical and data system

The pilot unit was powered by a Sorenson DCR 300-9B power supply capable of 300 V dc and 10 A output. The voltage, current and various incremental voltages of the pilot unit were monitored and logged manually as well as with a data acquisition unit featuring a personal computer running LabTech Notebook software and a ADAC A/D voltage measurement card and line isolators.

The pore fluid from the treatment zones was analyzed periodically for specific conductance and pH. Conductance was measured using a Cole Parmer model 19101 specific conductance meter. A Corning model 140 meter and Orion model 91 series electrode were used to measure pH.

The analysis of the model organic contaminant PNP involved extracting PNP from clay samples with 0.1N NaOH solution and measuring the level of PNP in solution by spectrophotometric absorption at 400 nm or by high performance liquid chromatography (HPLC). One extraction was sufficient to remove all PNP from clay. For carbon, which binds PNP much more tightly, the extraction solution contained 0.1N NaOH and 2 wt% methylene chloride, and repeated extractions were carried out to maximize PNP recovery.

Electro-osmotic flow rate for the kaolinite experiments was measured by diverting the recycle flow into a graduated cylinder or flask. A Turbo model Magmeter MG911/F3 flow meter was installed in the recycle line for the Paducah soil runs. The meter controller unit was equipped with a 0–5 V dc output which was connected to the data system. The meter calibration was checked in the lab at flow rates of 0, 60 and 500 ml h^{-1}.

2.4. Electrokinetic parameters

For each run, the electro-osmotic permeability can be calculated using the following equation:

$$Q = k_e(\Delta E)\, A \tag{1}$$

where Q is the volumetric flow rate by electro-osmosis ($cm^3\ s^{-1}$), k_e the coefficient of electro-osmotic permeability ($cm^2\ V^{-1}\ s^{-1}$), ΔE the voltage gradient applied across the soil mass ($V\ cm^{-1}$) and A the cross-sectional area perpendicular to flow (cm^2).

The coefficient of electro-osmotic transport efficiency, k_i, is by definition:

$$k_i = Q/I \tag{2}$$

where I is the current in A. Combined with Eq. (1) and with simple rearrangement, Eq. (2) becomes:

$$k_i = k_e/\lambda \tag{3}$$

where λ is the conductivity of the soil column (mho cm^{-1}). The transport efficiency k_i has the units of $cm^3\ A^{-1}\ s^{-1}$ and reflects the efficiency of current usage for pumping water through the soil column.

2.5. Energy consumption calculations

Energy consumption is an important factor in the overall economics of electroremediation processes and needs to be carefully optimized. The following discussion will cover two situations: the conventional electrokinetic configuration with two electrodes, and the Lasagna configuration containing a number of treatment zones between the two electrodes. The main difference in the two configurations is that the energy usage in the Lasagna configuration is closely tied to the treatment zone spacing instead of electrode spacing.

2.5.1. Conventional electrokinetic operation

Consider the simple case of two parallel plate electrodes of area A and separated by a distance L. The relevant equations follow.

$$P = EI = E^2/R = (\Delta E L)^2/R \tag{4}$$

$$R = \rho L/A \tag{5}$$

$$t = L/(k_e \Delta V) \tag{6}$$

$$V = LA \tag{7}$$

$$W = Pt/V \tag{8}$$

where

P	power consumption, kW
E	applied voltage, V
I	current, A
R	resistance of soil between the two electrodes, ohm
ΔE	voltage gradient, V m^{-1}
ρ	soil resistivity, ohm m
L	electrode spacing, m
A	cross-sectional of soil in contact with electrodes, m^2
t	time taken for water transported from anode to cathode, s
V	volume of soil between the two electrodes, m^3
W	specific energy consumed, kwh m^{-3} per pore volume

It can then be shown that

$$W = \frac{L \Delta E}{\rho k_e} \tag{9}$$

Eq. (9) shows clearly that the energy consumed as defined (kwh per m^3 of soil treated per pore volume of the soil between the electrodes) is proportional to the voltage

gradient *as well* as electrode spacing. This is important since extrapolation of energy usage for large-scale field operations based on bench/pilot data can be way off if the difference in electrode spacing is not corrected for. Additionally, for the same electrode spacing the energy usage, hence the cost of treatment, increases proportionally with the voltage gradient applied, that is, lower voltage gradient is more energy efficient. This fact is a consequence of power varying with the square of voltage, whereas electrokinetic transport (electro-osmosis/electromigration) is linearly proportional to the voltage gradient.

2.5.2. Lasagna configuration

In the Lasagna process the transport distance required is not from electrode to electrode but from one treatment zone to the next. Consider a number of treatment zones equally spaced at a distance d between the electrodes. The treatment time per pore volume of liquid transport between two adjacent treatment zones is

$$t_{TZ} = \frac{d}{k_e \Delta E} \tag{10}$$

The specific energy consumption defined as kwh per m^3 of soil treated per pore volume between adjacent treatment zones is then

$$W = \frac{P t_{TZ}}{V} = \frac{d \Delta E}{\rho k_e} \tag{11}$$

Which is identical to Eq. (9) but the relevant distance is now the treatment zone spacing instead of the electrode spacing. Everything else being equal, the energy usage for remediation will be lower for smaller treatment zone spacing. From an overall cost standpoint, the lower energy consumption for more closely spaced treatment zones is balanced by higher material and installation costs due to the larger number of treatment zones required.

3. Results and discussion

Scale-up experiments using the pilot unit were carried out first with kaolinite as the model soil whose electrokinetic characteristics have been well studied in our laboratory as well as by other researchers. Subsequent studies were then conducted using the actual Paducah soil.

3.1. Kaolin clay

3.1.1. Electrokinetic characteristics—bench / pilot comparison

A large number of experiments were conducted with bench-top electro-osmosis units to provide data for designing the pilot unit. Bench-scale results for kaolinite have been

Table 2
Comparison of pilot unit to bench-top units for kaolin clay

Parameter	Unit	Bench-top	Pilot	Ratio pilot/bench
Length (include sand zones)	cm	18	118.1	7
Cross section area	cm^2	81	2600	32
Pore volume/soil zone	cm^3	300	56000	187
Treatment zone spacing	cm	6	35.56	6
Voltage gradient	$V\ cm^{-1}$	1	1	1
Current density	$A\ m^{-2}$	0.57	0.37	0.7
EO conductivity (k_e)	$cm^2\ V^{-1}\ s^{-1}$	2.5×10^{-5}	1.7×10^{-5}	0.68
Energy consumption	kwh per m^3 pv	10	51	5.1
Resistivity	ohm cm	19100	27300	1.4

Both units had 2 steel electrodes/sand–carbon zones and 2 sand–carbon treatment zones evenly spaced between the electrodes.

reported elsewhere [10]. The pilot unit was 7 times longer, 32 times larger in cross sectional area, and 187 times more volume between the two treatment zones.

The kaolinite pilot unit was operated at constant voltage (1 V per cm voltage gradient) for 36 days with one polarity reversal. In the first pass, liquid flow equivalent to 0.87 pore volume of the center zone was obtained in 19 days. The polarity was then reversed for 17 days passing 1.0 pore volume. The results are shown in Table 2, which also lists the corresponding data for a typical bench-top run for comparison. Average liquid flow rate for the entire pilot run was 120 $cm^3\ h^{-1}$, equivalent to an average electro-osmotic permeability (k_e) of $1.7\times10^{-5}\ cm^2\ V^{-1}\ s^{-1}$.

The average transport efficiency (k_i) was 0.36 $cm^3\ A^{-1}\ s^{-1}$; and the total energy consumption was 58 kwh m^{-3} per pore volume (pv) of liquid. Note that the energy consumption in kwh m^{-3} pv should be proportional to the treatment zone spacing (Eq. (11)), which explains the 5× increase in the power usage for the pilot unit vs. bench due to the corresponding 6-fold increase in the zone spacing. Table 2 shows that electro-osmosis in the Lasagna configuration scales up reasonably well for kaolinite clay.

3.1.2. PNP removal

The effectiveness of the Lasagna process for removing PNP as the model organic contaminant from clay in the pilot unit was studied. Being a weak acid PNP dissociates in aqueous solution as a function of pH according to the following:

$$PNP \Leftrightarrow PNP^- + H^+$$

The pK_a value for PNP is 7.15 [23]. In the non-ionized (neutral) form, PNP should move with the water. In the ionized form, PNP is negatively charged and its electromigration towards the anode, opposite to the direction of electro-osmotic flow, is probably dominating. Extensive studies with the bench electro-osmotic cell showed that PNP was primarily transported along with the water [10].

Five sausage-like units of PNP contaminated clay were placed in the center section of the pilot unit, four horizontally and one vertically as described in Section 2. The initial

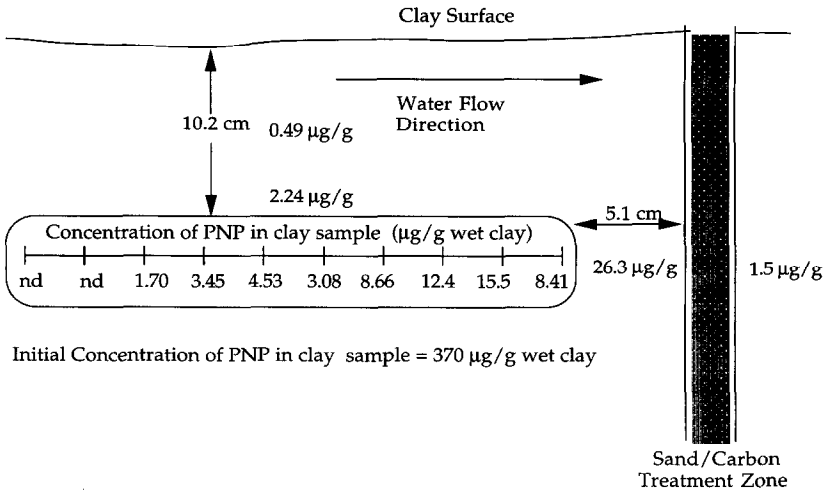

Fig. 5. Residual PNP concentration in a horizontal sausage after 1 pore volume. Initial PNP concentration was 370 μg per g wet clay.

PNP concentration was 370 μg PNP per g wet clay. The unit was operated for 14 days in one direction resulting in a 0.94 pore volume of water exchange in the center clay section. A single horizontal PNP contaminated sausage and some kaolinite soils surrounding the sausage were removed and analyzed for PNP. The results showed that over 98% of the loaded PNP had been removed from the sausage in this single pass. A maximum PNP concentration of 15 μg per g wet clay was detected at the downstream end of the sausage, with decreasing PNP concentration toward the upstream end, which contained no PNP (Fig. 5).

The PNP contaminated sausage was returned to the unit. Electrical polarity was then reversed and maintained for 25 days sweeping an additional 1.6 pore volume. After that, all sausages, as well as representative samples from the center clay zone and the complete sand/carbon treatment zones were extracted and analyzed for PNP. No detectable (< 10 ppb) amount of PNP was found in any clay samples. All the PNP recovered was from the carbon in the center treatment zones. Of the PNP recovered, 91% was found in the downstream treatment zone illustrating the efficiency of the first pass. However, only 55% of the estimated PNP loaded was recovered in the treatment zones. Loss of PNP through evaporation is unlikely due to its extremely low volatility: Henry's constant $= 4.15 \times 10^{-10}$ atm m^3 mol^{-1} [24]. Close to 100% PNP recovery was routinely obtained in bench-scale units [10], where PNP loading was typically at 100 mg PNP per g carbon. The low PNP loading in the pilot unit (< 5 mg PNP per g carbon) made it difficult to extract all the adsorbed PNP. Due to the large amount of carbon used, a small residual of PNP on the carbon would result in a relatively large fraction of PNP not recovered. Despite the low mass balance, the fact that PNP was completely removed from the clay zones is indicative of the effectiveness of the technology for cleanup of organic contaminants like PNP.

Table 3
Comparison of pilot unit to bench-top units for Paducah soil

Parameter	Units	Bench-top	Pilot	Ratio Pilot/Bench
Length (include carbon zones)	cm	18	118	6.6
Cross section area	cm^2	81	3030	37
Pore volume/soil zone	cm^3	173	43130	249
Treatment zone spacing	cm	6	36	6
Voltage gradient	$V\ cm^{-1}$	1	1	1
Current density	$A\ m^{-2}$	1.1	2.0	1.8
EO conductivity (k_e)	$cm^2\ V^{-1}\ s^{-1}$	5.0×10^{-6}	$(5.6\text{--}10.6)\times10^{-6}$	1.1–2.1
Energy consumption	kwh per m^3 pv	24	200	8.3
Resistivity	ohm cm	4700	5100	1.1

Configuration: 2 steel electrodes/GAC zones; 2 GAC treatment zones evenly spaced between the electrodes.

3.2. Paducah soil

3.2.1. Electrokinetic characteristics—bench / pilot comparison

Paducah soil was used to study the electrokinetic characteristics of a real soil. As with kaolinite, many bench-top experiments were conducted prior to the pilot runs described here. Parameters monitored during these runs included soil temperature, pH, conductivity, and ions profiles. With two treatment zones in the center, the Paducah soil pilot unit was nearly 7 times longer, 37 times larger in cross sectional area, and 250 times more pore volume per soil zone than the bench-scale unit (Table 3). Prefabricated treatment zones contained 100% GAC instead of a mixture of sand and carbon as in the kaolinite experiments.

The Paducah soil pilot unit was operated at constant voltage for a total of 44 days with one polarity reversal. In the first pass, liquid equivalent to 0.71 pore volume of the center zone flowed in 21 days. The polarity was then reversed for 23 days passing 1.5 pore volumes. The average electro-osmotic permeability (k_e) for the first pass was $5.6\times10^{-6}\ cm^2\ V^{-1}\ s^{-1}$, comparable to the bench-scale data, but was much higher ($10.6\times10^{-6}\ cm^2\ V^{-1}\ s^{-1}$) for the reversed pass. The reason for this large difference is not clear. We suspected that the increased soil moisture content of this fairly dry soil (19% moisture) may have played a major role in the observed difference. The average transport efficiency (k_i) was $0.22\ cm^3\ A^{-1}\ s^{-1}$, and the total energy consumption was 200 kwh m^{-3} per pore volume of liquid, about 4 times that of kaolinite. Table 3 shows that the Paducah soil appears to scale up reasonably well with respect to energy consumption, which should be proportional to the treatment zone spacing (Eq. (11)).

3.2.2. Bipolar effects

With the treatment zones containing 100% activated carbon, which is electrically conducting, there was the possibility of them acting as bipolar electrodes due to the applied electric field. That is, the side of the carbon zone facing the anode could behave like a cathode (which would generate OH^- and release hydrogen), and the other side like an anode (which would generate H^+ and release oxygen). Evidence for bipolar effects in terms of voltage distribution and pH was shown in Fig. 6. Voltage drop

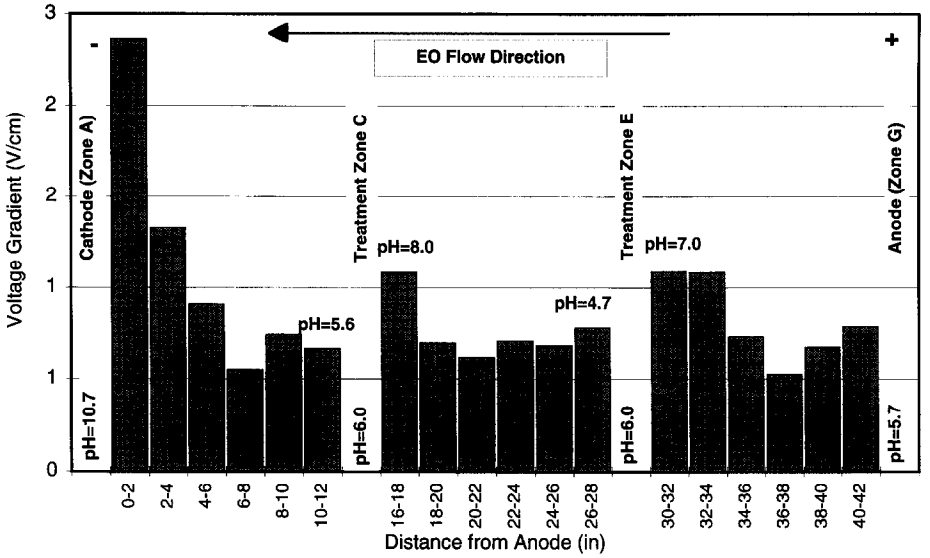

Fig. 6. Voltage gradient and pH profiles for Paducah soil in pilot unit with two GAC treatment zones. Overall applied voltage gradient was 1 V cm^{-1}.

typically tends to be higher near the cathode and lower near the anode [10], a pattern observed for the two treatment zones in this case. The pH of the soil on the "anode" sides of the treatment zones were low, and the pH on the "cathode" sides were high, consistent with pH characteristics of the electrodes.

3.2.3. Larger treatment zone spacing

The pilot unit was packed with fresh Paducah soil and the Monsanto Hydroway® treatment zones in a configuration that closely resembled the field design. A single treatment zone in the center of the unit and two electrode treatment zones were used. The Hydroway® zones were now spaced 53.3 cm apart. The unit was initially operated at 0.5 V cm^{-1}, which ran stably in one direction for 105 days with an average electro-osmotic permeability (k_e) of 1.1×10^{-5} cm^2 V^{-1} s^{-1}. Apparently, at this low voltage gradient the recycle of the cathode effluent back to the anode side was sufficient to stabilize the electro-osmosis process without the need for polarity reversal. Fig. 7 shows the values for flowrate and current during the three months of operation.

3.2.4. Conductivity and pH

The pH and specific conductance of the cathode effluent and of the water in the treatment zones were monitored during the course of operation. Within a few days, the specific conductance of the fluid in the cathode zone rose sharply. Ions analysis showed that this increase in solution conductivity was due to the presence of Na^+ (Fig. 8). Sodium ion apparently moved faster than the water and accumulated in the cathode region. The water recycle scheme of the Lasagna process provides a means for cations transported by electromigration to the cathode to be brought back to the anode zone where they could be reintroduced into the soil. After a few days of operation, the anode

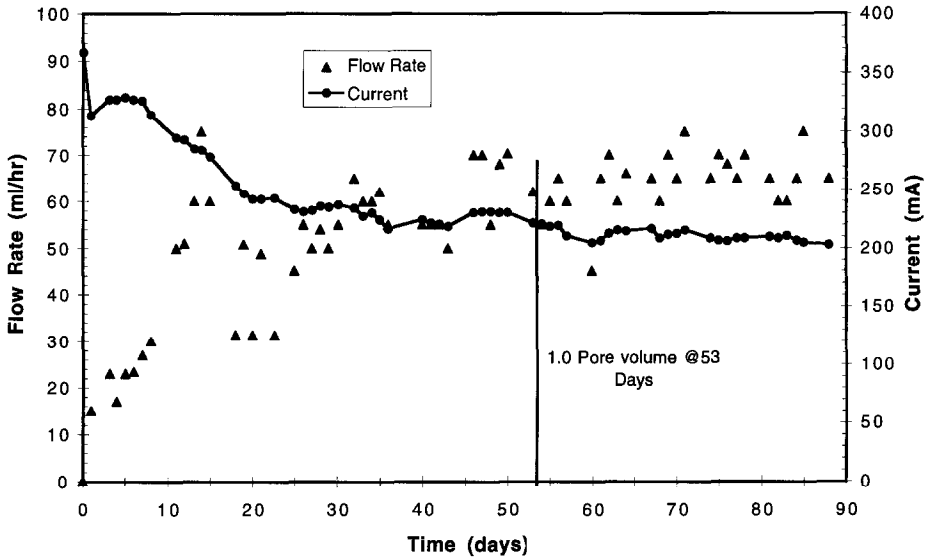

Fig. 7. Flowrate and current vs. time for a pilot run with Paducah soil; voltage gradient = 0.5 V cm^{-1}.

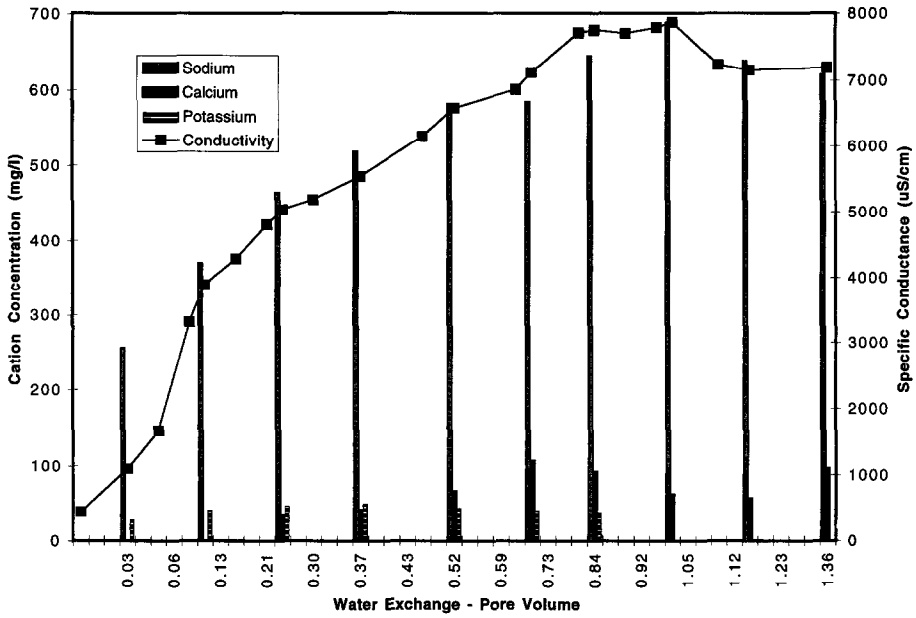

Fig. 8. Cations and solution conductivity of the cathode-zone fluid.

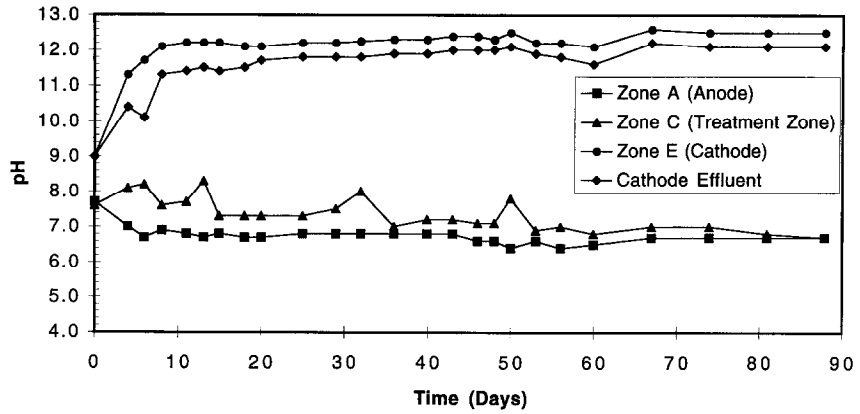

Fig. 9. pH of anode, cathode and treatment zone fluids vs. time for pilot run with 1 GAC treatment zone.

pH decreased from near neutrality to about 6 while the cathode pH effluent increased to over 12. The near neutral pH at the anode is thought to be partially due to the oxidation of the iron anode taking place preferentially over the electrolysis of water according to the following reactions with E_0 as the standard potential at 25°C:

$$Fe^0 \rightarrow Fe^{2+} + 2e^- \quad E_0 = +0.44\,V$$

$$2H_2O \rightarrow O_2 + 4H^+ + 4e^- \quad E_0 = -1.23\,V$$

This is consistent with the presence of rust in the anode solution. Most of the iron in solution did not seem to make it to the soil; most of it appeared to precipitate, probably as iron hydroxide, in the carbon zone in front of the anode. The pH of the anode solution was also neutralized by the high pH of the recycled cathode effluent. The pH in the center treatment zones did not vary much after the initial decrease from the starting pH of about 8 to a pH between 6 and 7 (Fig. 9). The specific conductance of water in the treatment zones showed some fluctuations between 300 to 500 $\mu S\ cm^{-1}$.

3.2.5. Effects of voltage gradient

The relationship between the applied voltage gradient and the corresponding electro-osmotic flowrate was studied from about 1 V cm^{-1} down to below 0.1 V cm^{-1}. The electro-osmotic flowrate was found to vary quite linearly with the applied voltage gradient (Fig. 10). Extrapolation of the fitted line indicates that the flow would stop at a voltage gradient of 0.06 V cm^{-1}, or an overall voltage of about 7 V. This "threshold voltage" for the pilot unit probably reflects the voltages required to drive the electrode reactions and the overvoltages associated with the particular experimental setup. The results suggest that for a much larger setup (field-scale) where the overall voltage applied will be much higher than 7 V, electro-osmosis can be operated efficiently at very low voltage gradients. For example, a 0.1 V per cm gradient for a 10 m electrode spacing would result in a total voltage of 100 V. The low voltage gradient is attractive in field operations due to less severe soil heating (described in the next section). Another benefit of low voltage operations is less energy consumption per unit of water

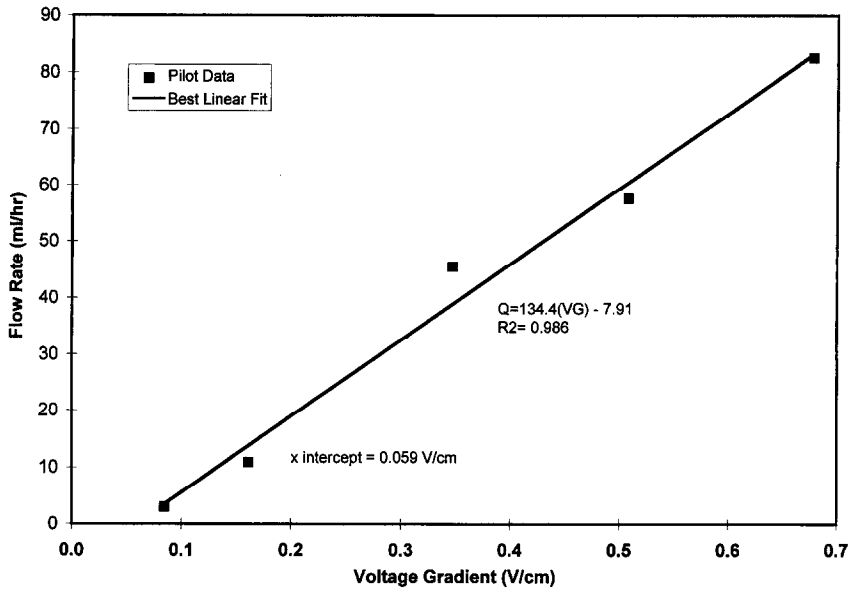

Fig. 10. Effect of voltage gradient on electro-osmotic flow for Paducah soil.

transported electro-osmotically. This is a consequence of the fact that power consumption varies with the square of the applied voltage whereas transport rate by electro-osmosis and electromigration is proportional to the voltage gradient, as shown in Section 2.5.

3.2.6. Soil heating

Soil heating will occur in the use of electrokinetics for soil remediation due to the electrical input. While heating has not been an issue in laboratory studies, our modeling work discussed in the next section suggests that in field-scale applications thermal effects of Joule heating will be significant. Under steady-state conditions, the energy supplied to the soil by Joule heating is balanced by thermal conduction of the energy to the boundaries of the soil system. As the size of the treated soil increases, the surface area to volume ratio decreases, and the characteristic length for heat conduction increases. This leads to a maximum steady-state temperature rise in the soil that varies with the square of the characteristic length of the region. For instance, in a one-dimensional geometry in which electrodes maintained at temperature T_0 form the boundary conditions, the maximum steady-state temperature in the center of the domain is $T_0 + \sigma E^2 L^2/8k$, where σ is the electrical conductivity, E the applied field, L the electrode spacing, and k the thermal conductivity of the soil. Therefore, field experiments, which may easily be a factor of ten larger than laboratory experiments, might be expected to have temperature rises on the order of 100-fold larger than the similar laboratory experiment. Temperature rises as a function of the voltage gradient applied were measured to assess the importance of this effect and to provide data for the modeling effort.

Fig. 11 shows the core soil temperature of the pilot unit (at the center of the soil mass) as a function of the applied voltage gradient. At 0.5 V cm^{-1}, the core temperature

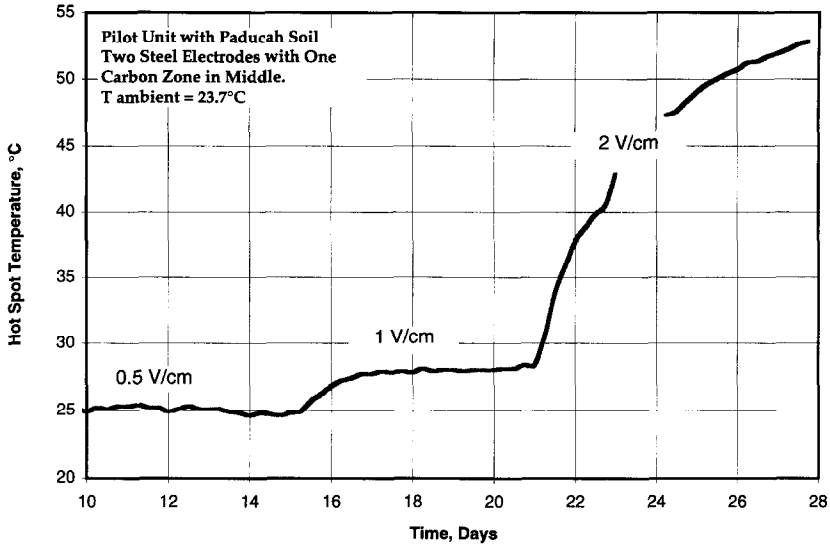

Fig. 11. Effect of voltage gradient on maximum soil temperature in the pilot unit.

only went up to almost 25°C, an average of 1.1° above the ambient temperature of 23.7°C. When the voltage gradient was increased to 1.0 V cm^{-1}, the core temperature increased over several days to an average of 4.8°C over ambient. The voltage gradient was then doubled again to 2.0 V cm^{-1}. This caused a dramatic increase in soil core temperature, which within one week was approaching 53°C, a temperature rise of almost 30°C! The temperature rise appears to be roughly proportional to the square of the voltage gradient, consistent with the power input varying with the square of the applied voltage.

3.3. Modeling of thermal effects

The significant temperature rises observed in the pilot experiments prompted the development of the following mathematical model describing Joule heating and heat transfer by conduction and convection [13].

The coupled equations describing the electric and temperature fields are: Charge conservation:

$$\nabla \cdot \sigma(T)\nabla\phi = 0 \tag{12}$$

Electro-osmotic and hydraulic flow through porous media:

$$u = -\frac{k_e(T)}{n}\nabla\phi - \frac{k_h}{n\mu}\nabla p \tag{13}$$

Energy conservation:

$$\frac{\partial T}{\partial t} = \frac{k}{\rho c}\nabla^2 T - nu\frac{\rho_w c_w}{\rho c}\cdot\nabla T + \frac{\sigma(T)}{\rho c}\|\nabla\phi\|^2 \tag{14}$$

Table 4
Model parameters

Parameter	Value
Porosity, n	0.4
Thermal conductivity, k	1.2 W m^{-1} K^{-1}
electrical conductivity, σ_0(20°C)	0.024 S m^{-1}
Pore fluid viscosity, μ(20°C)	0.001 kg m^{-1} s^{-1}
Soil density, ρ	1970 kg m^{-3}
Soil heat capacity, c	1870 J kg^{-1} K^{-1}
Water density, ρ_w	1000 kg m^{-3}
Water heat capacity, c_w	4180 J k^{-1} K^{-1}
Electro-osmotic permeability, k_e(20°C)	1.2×10^{-9} m^2 V^{-1} s^{-1}

where ϕ is the electric potential, σ the electrical conductivity, u the pore fluid velocity, k_e the soil electro-osmotic permeability, k_h the intrinsic soil hydraulic permeability, μ the pore water viscosity, n the soil porosity, T the soil temperature, ρ the soil density, c the specific heat of the soil, ρ_w the pore water density, c_w the pore water specific heat, and k the thermal conductivity. These parameters are listed in Table 4.

Eq. (4) makes several simplifying assumptions regarding charge transport in the soil. First, there are no capacitive effects, which should be the case with a DC electric field. Second, charge is transferred predominantly by ionic migration, so that convection in the charged double layer at the soil particle/pore liquid interface and current carried by diffusion of ions are negligible. And third, the electrical conductivity, to first order, is a function of temperature only. This final assumption is the most limiting in light of several investigations [14–18] which have examined the transport of ions in electrokinetic applications, both experimentally and theoretically, and have shown that electrical conductivity becomes a strong function of position as ions get redistributed by the electric field and electrode reactions. However, in soils with moderate buffering capacity it can be shown [19] that this effect can be neglected in certain cases, including the laboratory tests simulated in this work.

Because both fluid viscosity and electrical conductivity are very sensitive to temperature, their temperature dependence has been incorporated in this model. The viscosity dependence is reflected the electro-osmotic permeability, k_e, which varies inversely with viscosity, according to the Helmholtz–Smoluchowski equation [20]. That is, the effects of temperature on the zeta potential, dielectric constant, and solubility of species are ignored. The following expression for the temperature dependence of viscosity of water [21] was used to estimate the temperature dependence of the electro-osmotic permeability:

$$\log_{10}\left(\frac{k_e(T)}{k_e(20°C)}\right) = -\log\left(\frac{\mu(T)}{\mu(20°C)}\right)$$

$$= \frac{1.3273(T-20°C) + 0.001053(T-20°C)^2}{(T-20°C)+125} \qquad (15)$$

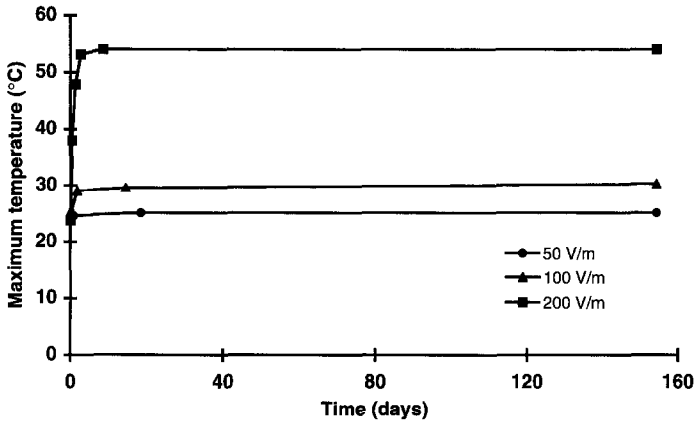

Fig. 12. Model prediction of the maximum soil temperatures for three voltage gradients.

Laboratory experiments determined that the temperature dependence of soil electrical conductivity can also be expressed as a function of fluid viscosity [13]. The inverse relation between electrical conductivity and fluid viscosity is consistent with the behavior of ionic aqueous solutions [22]. Thus the temperature dependence of conductivity was also expressed in terms of fluid viscosity as

$$\sigma(T) = \sigma(20°\mathrm{C})\frac{\mu(20°\mathrm{C})}{\mu(T)} \tag{16}$$

A two-dimensional rectangular geometry (1.2 m wide × 0.45 m deep) was used to represent the experimental apparatus used in these experiments. The left side of the rectangle was the anode and the right side was the cathode. The boundary conditions for the electric field were $\phi(\text{anode}) = \phi_0$ (60, 120 or 240 V) and $\phi(\text{cathode}) = 0$. The top and bottom sides of the rectangle were electrically insulated. The thermal boundary conditions are constant temperature of 23.7°C at all four sides of the domain. The parameters used in the example computer simulation are given in Table 4. The model was executed using FIDAP®, a commercial finite element computational fluid dynamics package.

The thermal model was run for three applied voltages, 60, 120, and 240 V. Three cases are analyzed for maximum soil temperature, power and flow rate. The calculated maximum temperatures for these cases are shown in Fig. 12. For this geometry, the warmest region lies in the center of the domain, and from the symmetry of the temperature field (Fig. 13), it can be concluded that electro-osmotic convection is unimportant in heat transfer. This may not be the case if arrays of cylindrical electrodes are used. In such cases, maximum temperature may occur near the electrodes where the current is concentrated.

From Fig. 12 it can be observed that the temperature rises begin relatively rapidly and then converge toward a steady value. The time-scale for thermal diffusion across the narrow dimension of the geometry (in this case 0.45 m from top to bottom) is given by $L^2\rho c/k$, and is of the order of 7 days for the highest voltage gradient. Since the electrical

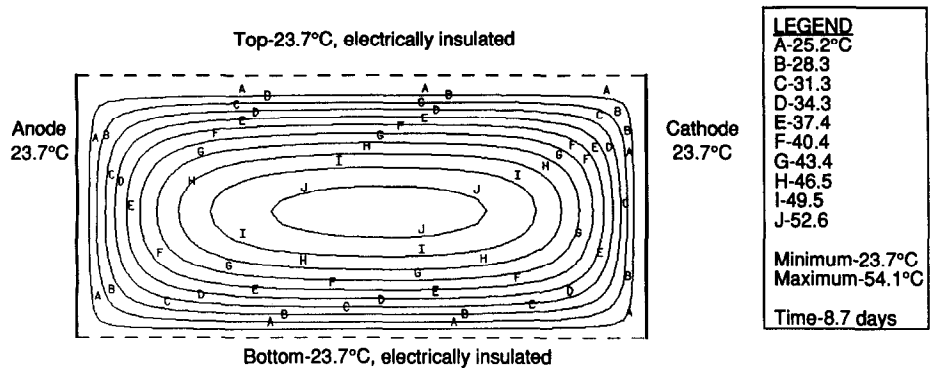

Fig. 13. Computational geometry and isotherms for 240 V case. Anode–cathode distance is 1.1 m; top–bottom distance is 0.45 m. Solution is shown for 8.7 days, at which time the temperature field was essentially steady state.

conductivity of the soil increases with temperature, the amount of power increases with time in these constant applied voltage experiments. Because the relative change in power from initial conditions increases with applied field, the time required to reach a steady-state temperature distribution increases with increasing field. This behavior is seen in the model predictions and, more clearly, in the experimental measurements shown in Fig. 11. Here it is observed that the time to reach steady temperature was about 2 days at 1 V cm^{-1} and about 8 days at 2 V cm^{-1}. A more important observation regarding thermal diffusion time is that in field applications in which the characteristic dimension is, say, 10 m, the steady state temperatures would not be reached until 3500 days, or well after the remediation was completed.

The steady state temperature rises were 1.4, 6.6, 30.3°C for the 60, 120, and 240 V cases respectively. This compares well with experimental measurements of 1.3, 4.9, and ~ 30°C for the respective conditions. The fact that the measured temperature rises are slightly smaller than the model predictions may be attributable partly to inaccuracies in input properties and partly to the use of a two-dimensional model, which resulted in less effective heat transfer area, to represent a three-dimensional situation. The thermal conductivity of 1.2 W mK^{-1} was the only parameter chosen to achieve a good fit with experimental data; other properties listed in Table 4 were measured independently. The fact the best fit to the data was achieved with a thermal conductivity value typical of moist soils supports the assumptions made in the model. The factor of 4.7 between the temperature rise for the 120 V case and the 60 V case is slightly higher than the order of magnitude scaling which predicts that the temperature rise will be proportional to the electric field squared. The nonlinearity of the system, however, is more apparent when comparing the 60 and 240 V cases. The ratio of temperature rises predicted in the simulations was 21.6 (the ratio of the corresponding temperature rises in the experiments was 23.1) compared to the factor of 16 that would be expected in a linear system.

The increased temperature rise at higher voltages is attributable to the temperature dependency of the electrical conductivity. As the conductivity increases, the V^2/R losses increase, because the system resistance goes down. Therefore the power supplied

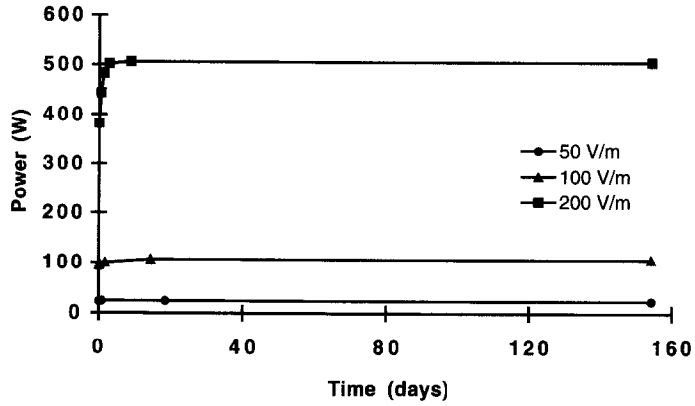

Fig. 14. Model prediction of power input vs. time for three voltage gradients.

to the soil increases with time as shown in Fig. 14. The transient behavior of the applied power is clearly dependent on the control strategy. If, instead of constant voltage, a constant current were maintained, the power (I^2R) would decrease with time as a result of decreasing resistance. In fact, operating at constant current in field-scale applications has the important advantage of heating the soil relatively quickly early in the process, and approaching the steady state operating conditions faster than a constant voltage control system. As with the temperature rise, nonlinearity is seen in the relation between applied voltage and electro-osmotic flow (Eq. (15)). The ratio of the flow rate in the 240 V case to the 60 V case is 5.5, or 38% larger than if the electro-osmotic permeability were independent of temperature.

4. Summary and conclusions

A novel integrated in situ remediation technology, called Lasagna™, is being developed coupling electrokinetics with in situ treatment zones. Experiments were conducted with kaolinite and an actual soil in units ranging from bench-scale containing kg-quantity of soil to a pilot-scale containing about half a ton of soil having various treatment zone configurations. The obtained data support the feasibility of scaling up this technology with respect to electrokinetic parameters such as electro-osmotic permeability as well as energy consumption. The latter was found to be approximately proportional to the treatment zone spacing, a characteristic of the Lasagna process that may not be obvious but is consistent with theoretical calculations. The removal of the model organic compound PNP from the soil was also very efficient (98% in one pass) in the pilot unit, even though a mass balance of only 55% was obtained. This relatively low mass balance is believed to be due to the very low loading of PNP in terms of mg PNP per g of total clay soil or carbon in the system, which could magnify percentage loss due to residual PNP left on the soil and/or on the carbon. A mathematical model was developed that was successful in predicting the temperature rises in the soil. The

information and experience gained from these experiments along with the modeling effort enabled us to successfully design and operate a larger field experiment at a DOE clay site contaminated with trichloroethylene.

Acknowledgements

The authors would like to thank Jay Wendling of Monsanto for PNP HPLC and ion chromatography analysis. Special thanks go to the following members of the Monsanto shop services and instrument support team for their help in constructing the pilot unit and data system: Kevin Deppermann, Alan Jackson, John Mathews, and Marvin Denison. This work was supported in part by the US Department of Energy through contract number 21-94MC31185.

References

[1] L.J. Casagrande, Boston Society of Civil Engineers 39 (1952) 51-83.
[2] A.P. Shapiro, P. Renaud, R. Probstein, Preliminary studies on the removal of chemical species from saturated porous media by electro-osmosis, in: Physicochemical Hydrodynamics, Vol. 11, No. 5/6, 1989, pp. 785-802.
[3] J. Hamed, Y.B. Acar, R.J. Gale, ASCE 112 (1991) 241-271.
[4] C.J. Bruell, B.A. Segall, J. Environ. Eng. 118 (1) (1992) 68-83.
[5] B.A. Segall, C.J. Bruell, J. Environ. Eng. 118 (1) (1992) 84-100.
[6] Y.B. Acar, H. Li, R.J. Gale, ASCE 118 (11) (1992) 1837-1852.
[7] A.P. Shapiro, R.F. Probstein, Environ. Sci. Technol. 27 (1993) 283–291.
[8] R. Lageman, Electroreclamation—applications in The Netherlands, Environ. Sci. Technol. 27 (13) (1993) 264–280.
[9] Y.B. Acar, A.N. Alshawabkeh, Principle of electrokinetic remediation, Environ. Sci. Technol. 27 (13) (1993) 2638–2647.
[10] S.V. Ho, P.W. Sheridan, C.J. Athmer, M.A. Heitkamp, J.M. Brackin, D. Weber, P.H. Brodsky, Integrated in situ soil remediation technology—the Lasagna process, Environ. Sci. Technol. 29 (10) (1995) 2528–2534.
[11] P.H. Brodsky, S.V. Ho, US Patent No. 5,398,756, March 1995. The term Lasagna™ has also been trademarked by Monsanto.
[12] L. Murdoch, Some recent development in delivery and recovery: hydraulic fracturing and directional drilling, in: Proceedings of ETEX'92—The 2nd Annual Environmental Technology Exposition and Conference, Washington, DC, USA, April 7–9, 1992.
[13] A.P. Shapiro, D.S. Schultz, Emerging technologies in hazardous waste management VII, in: 1995 Extended Abstracts for the Special Symposium, Atlanta, GA, American Chemical Society, p. 457.
[14] A.P. Shapiro, P.C. Renaud, R.F. Probstein, PhysicoChem. Hydrodyn. 11 (1989) 785.
[15] A.N. Alshawabkeh, Y.B. Acar, J. Environ. Sci. Health A 27 (7) (1992) 1835.
[16] G.R. Eykholt, D.E. Daniel, J. Geotech. Eng. 120 (5) (1994) 797.
[17] R.A. Jacobs, J. Environ. Sci. Health A 29 (9) (1994) 1933.
[18] R.E. Hicks, S. Tondorf, Environ. Sci. Technol. 28 (12) (1994) 2203.
[19] R.A. Jacobs, AIChE J. (1996), in press.
[20] R.F. Probstein, Physicochemical Hydrodynamics, An Introduction, 2nd ed., John Wiley and Sons, Inc., New York, 1994, p. 197.
[21] R.C. Weast (Ed.), Handbook of Chemistry and Physics, The Chemical Rubber Co., Cleveland, 1972, p. F-36.
[22] R.W. Gurney, Ionic Processes in Solution, Dover Publications, New York, 1953, p. 69.
[23] P.J. Pearce, R.J.J. Simkins, Can. J. Chem. 46 (1968) 241–248.
[24] J. Hine, P.K. Mookerjee, J. Org. Chem. 40 (1975) 292–298.